GSA DATA REPOSITORY 2011142

Multiple phases of carbon cycle disturbance from Large Igneous Province formation at the Triassic-Jurassic transition

M. Ruhl * and W.M. Kürschner

Palaeoecology, Laboratory of Palaeobotany and Palynology, Institute of Environmental Biology, Faculty of Science, Utrecht University, Budapestlaan 4, NL-3584 CD, Utrecht, Netherlands
*Corresponding author's e-mail: micharuhl@gmail.com

MARINE RECORD

The marine sequences of Tiefengraben and Eiberg (Austria; Figure 1 and 2 Main Text) are located in the palaeo-Eiberg basin, a marine sedimentary basin in between extensive carbonate platforms on the western Tethys passive margin (Kürschner et al., 2007). Both outcrops are closely spaced to the base Jurassic GSSP at Kuhjoch (Hillebrandt et al., 2008). The Tiefengraben sequence was deposited at the margins of the Eiberg basin while the Eiberg sequence originates from its central and deepest part (explaining higher sedimentation rates at Tiefengraben). Correlation of T-J transition sections in the Eiberg basin are well constraint, based on geochemical, palaeontological and lithological markers (Kürschner et al., 2007; Hillebrandt et al., 2008; Bonis et al., 2009; Hillebrandt and Krystyn, 2009; Ruhl et al., 2009; Bonis et al., 2010). The Eiberg sequence is in contrast to shallower sections in the basin, marked by marl deposition at the top of the Kössen Fm, allowing for high resolution $\delta^{13}C_{TOC}$ studies in the upper Rhaetian. This sedimentary interval is marked by relatively continuous $\delta^{13}C_{TOC}$ values of ~-26.5‰, with significantly lower values of ~-29.5‰ approximately 4 meters below the top of the Eiberg member (Kössen formation) (Figure 2 Main Text). It is further marked by even lower values of ~-31.5‰ at the end-Triassic extinction interval at the base of the Tiefengraben member (Kendlbach formation). Comparison of the marine records of the Eiberg basin to St Audrie's Bay in northwest Europe is relatively straightforward with distinct geochemical and biological correlation points (Kürschner et al., 2007; Ruhl et al., 2009; Bonis et al., 2010).

NON-MARINE RECORD

The upper Rhaetian Hauptton sequence in the southwestern end of the Germanic Basin (Wüstenwelsberg quarry, Germany; Figure 1 and 2 Main Text), is regarded as the continental equivalent of the marine *Contorta*-beds in the more central part of the basin (Bloos, 1990). Its grey organic rich clays directly succeed the fluviatile Haupt Sandstein. The Hauptton is marked by typical upper Rhaetian (Triassic) palynomorph assemblages, with high abundance of *Ricciisporites tuberculatus*, *Ovalipollis pseudoalatus* and *Vitreisporites bjuvensis* pollen

(Bonis et al., in press), similar and time-equivalent to the upper Rhaetian Westbury formation in St Audrie's Bay (Bachmann and Kozur, 2004; Bonis et al. 2010). The Hauptton is marked by gradually increasing $\delta^{13}C_{TOC}$ values, from ~-25 to ~-23‰ (Figure 2 Main Text). Significantly lower values of ~-27‰ coincide with organic rich deposits halfway the Hauptton. Three uppermost samples are Hettangian (Jurassic) in age, with palynomorph assemblages marked by a total absence of *Ricciisporites tuberculatus* and increased abundance of *Classopollis meyeriana* pollen (Bonis et al., in press) and ^{13}C depleted carbon isotope values of ~-26.5‰.

The studied sequence contains several leaf-bearing horizons with well preserved *Lepidopteris ottonis* leaves (Bonis et al., in press). Carbon isotope values of these leaves are around ~-26 to ~-27‰, which is typical for C_3 plants and inline with previous studies (Bocherens et al., 1993). A negative CIE in the $\delta^{13}C_{Leaves}$ record coincides with the observed ~2-3‰ negative CIE in $\delta^{13}C_{TOC}$. The observed amplitude is, however, smaller as no leaves were preserved at levels with most negative $\delta^{13}C_{TOC}$ values (Figure 2 Main Text).

STRATIGRAPHIC BACKGROUND

The duration of the Rhaetian stage and stratigraphic position of the Norian-Rhaetian and Rhaetian-Hettangian boundaries, were often adjusted with changing preference of biostratigraphic boundary markers. The proposed Global boundary Stratotype Section and Point (GSSP) for the base of the Rhaetian stage, at Steinbergkogel (western Tethys realm, Austria) (Krystyn et al., 2007), considers three potential boundary markers. The first two, based on the first occurrence (FO) of the *Misikella hernsteini* and *M. posthernsteini* conodont species assign most of the Sevatian 2 to the Rhaetian. The third option, based on the FO of *Vandaites stuerzenbaumi* ammonites, strongly reduces the duration of the Rhaetian. The studied interval in the western Tethys Eiberg Basin comprises the upper part of the Rhaetian *Choristoceras marshii* zone in the Kössen Fm and is succeeded by the Schattwald beds (which are part of the pre-*planorbis* beds) (Hillebrandt et al., 2007). The uppermost Rhaetian pre-*planorbis* beds directly preceed the base of the Jurassic, which is defined by the FO of *Psiloceras spelae tirolicum* ammonites at the base Jurassic GSSP at Kuhjoch (Hillebrandt et al., 2007). The Rhaetian stage in the Germanic Basin originally represented the upper Keuper. The lower, middle and upper Rhaetian division in the Germanic Basin heavily relies on lithostratigraphic units with particular guide fossils. The Rhaetian stage was later confined to the uppermost Arnstadt Fm/ lower-middle *Postera*-beds and the subsequent Exter Fm (Bachmann and Kozur, 2004). The middle to upper Rhaetian Exter Fm consists of the (Postera) Haupt Sandstein and the *Contorta* (Hauptton) and *Triletes* beds and is succeeded by the uppermost Rhaetian pre-*planorbis* beds. Correlation of the Rhaetian sub-stages in the Tethys realm and Germanic Basin is biostratigraphically however not well-established. The *Contorta*-beds may be related to the upper *C. marshii* ammonite zone in the Tethys Ocean (Lund, 2003) and the Westbury Formation (Fm) in the UK (Bachman and Kozur, 2004).

METHODS

Sample preparation and $\delta^{13}C_{TOC}$ measurements on marine and continental sediments from the Eiberg and Wüstenwelsberg section respectively, was performed according to Ruhl et al. (2009). Measurements were performed by Elemental Analyzer Continuous Flow Isotope Ratio Mass Spectrometry using a Fisons 1500 NCS Elemental Analyzer coupled to a Finnigan Mat Delta Plus Mass Spectrometer at the Geochemistry group of the Department of Earth Sciences, Utrecht University. Values are given in Figure 2 of the main-text and reported relative to Vienna PDB. The regular measurement of two internal laboratory standards for every 10 samples, demonstrate a standard deviation of < 0.071‰.

Duplicate and triplicate C-isotope measurements on bulk leaf material of single *Lepidopteris ottonis* leaf-pinnules from the Wüstenwelsberg section were similar to $\delta^{13}C_{TOC}$ measurements. *L. ottonis* leaves were extracted from the clayey sediments of the Hauptton and subsequently rinsed with demi-water. Remaining sedimentary particles still attached to the leaves, were removed by ultrasone (<30 seconds). Dupli- and triplicate measurements of specific *L. ottonis* leaves showed a relatively large standard deviation of ~0.07-0.5‰.

The required release of isotopically light carbon, to produce a ~2-3‰ negative CIE in the end-Triassic exogenic carbon pool, is computed with a simple mass balance calculation:

$$\delta^{13}C_{tot} * M_{Tot} = (\delta^{13}C_{oc} * M_{oc}) + (\delta^{13}C_{atm} * M_{atm}) + (\delta^{13}C_{add} * M_{add})$$

(with end-Triassic boundary conditions based on Beerling and Berner (2002); M = carbon mass in Gigaton; M_{oc} = oceanic carbon mass; M_{atm} = atmospheric carbon mass; M_{add} = carbon added to exogenic carbon pool; M_{tot} = total amount of carbon in exogenic carbon pool; $\delta^{13}C_{oc}$ = 0.6‰‰; M_{oc} = ~71248 Gt; $\delta^{13}C_{atm}$ = -6.4; M_{atm} = ~3000 Gt; $\delta^{13}C_{add}$ = -35 to -50‰).

δ^{13}C OF *LEPIDOPTERIS OTTONIS*

A more negative δ^{13}C composition of *L. ottonis* (Bocherens et al., 1993) and other Mesozoic leaves (Sun et al., 2003) could potentially reflect reduced water-stress in a swamp-like environment due to increased stomatal conductance and increased p_i/p_a values. Relatively wet palaeo-environmental conditions throughout the upper Rhaetian Hauptton in the Germanic Basin are however suggested by high relative abundance of spore producing plants (Bonis et al., in press). Minor changes in water-stress and stomatal conductance likely caused a negligible increase in carbon fractionation of *L. ottonis* plants in the studied section.

DATA REPOSITORY FIGURE DR1. Overview of Rhaetian sub-division in the Germanic Basin and Tethys and Boreal realm (Epicontinental Triassic International Symposium Guide, 1998; Channell et al., 2003; Kozur, 2003; Lund, 2003; Bachmann and Kozur, 2004; Nitsch, 2005; Hillebrandt et al., 2007; Krystyn et al., 2007; Warrington et al., 2008). Grey band shows suggested correlation of the Rhaetian (sub-) stage(s) based on carbon isotope stratigraphy.

DATA REPOSITORY FIGURE DR2. Three examples of *Lepidopteris ottonis* leaves from the Wüstenwelsberg section (collected by N.R. Bonis, J.H.A. van Konijnenburg-van Cittert, S. Schmeissner and G. Dütsch). Photos of different specimens are mutually scaled, scale-bar is in millimeters.

DATA REPOSITORY TABLE DR1. Bulk $\delta^{13}C_{TOC}$ and $\delta^{13}C_{Leaf}$ values of the Wüstenwelsberg section (Germanic basin/ Germany) and the Eiberg section (Eiberg basin/ Austria).

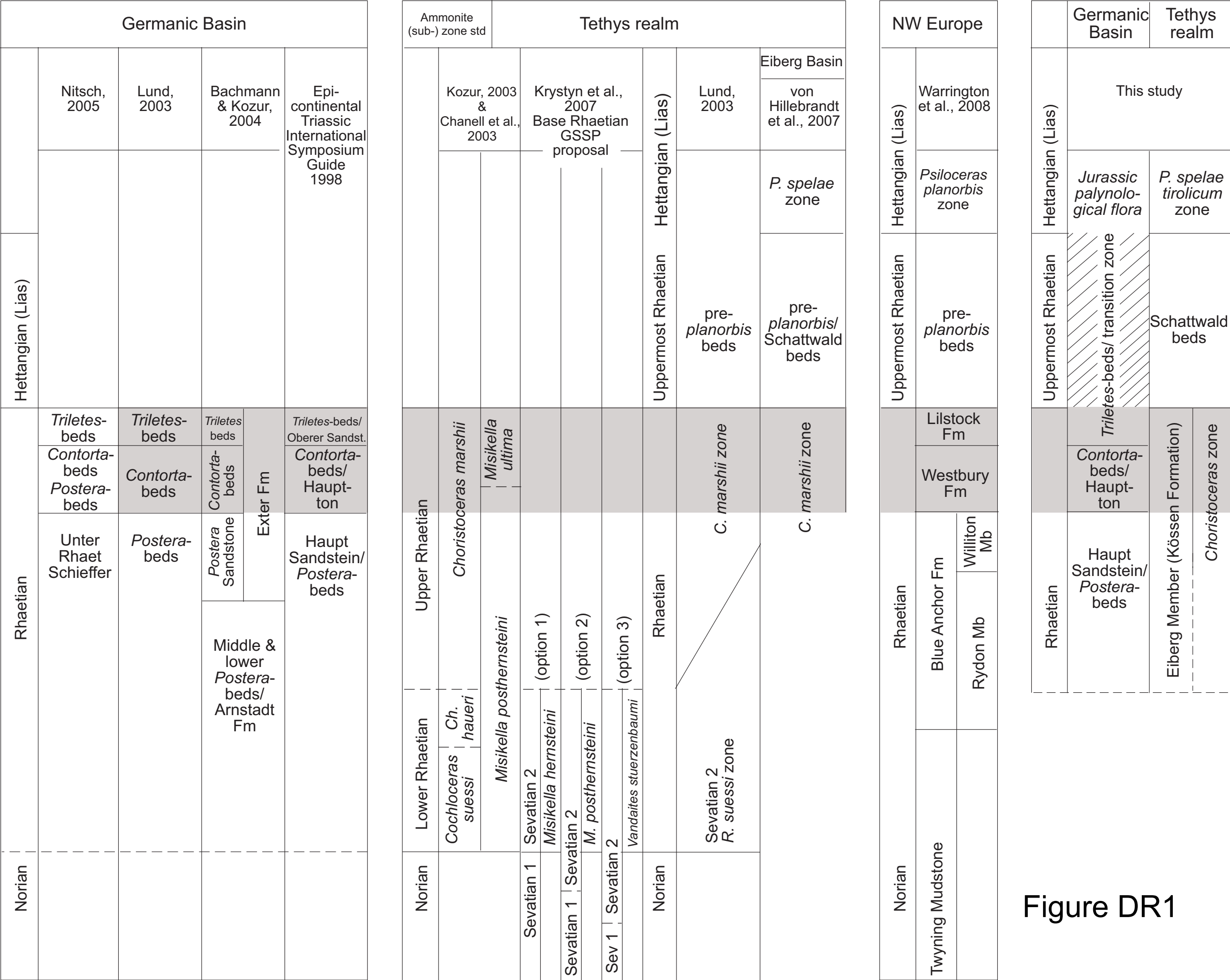
Germanic Basin
Nitsch, 2005
Lund, 2003
Bachmann & Kozur, 2004
Epi-continental Triassic International Symposium Guide 1998
Hettangian (Lias)
Rhaetian
Norian
Triletes-beds
Contorta-beds Postera-beds
Unter Rhaet Schieffer
Triletes-beds
Contorta-beds
Postera-beds
Triletes beds
Contorta-beds
Postera Sandstone
Exter Fm
Middle & lower Postera-beds/ Arnstadt Fm
Triletes-beds/ Oberer Sandst.
Contorta-beds/ Haupt-ton
Haupt Sandstein/ Postera-beds
Ammonite (sub-) zone std
Tethys realm
Kozur, 2003 & Chanell et al., 2003
Krystyn et al., 2007 Base Rhaetian GSSP proposal
Upper Rhaetian
Lower Rhaetian
Norian
Choristoceras marshii
Misikella ultima
Misikella posthernsteini
Ch. haueri
Cochloceras suessi
(option 1)
(option 2)
(option 3)
Sevatian 2
Misikella hernsteini
Sevatian 1
Sevatian 2
M. posthernsteini
Sevatian 1
Sevatian 2
Vandaites stuerzenbaumi
Sev 1
Hettangian (Lias)
Uppermost Rhaetian
Rhaetian
Norian
Lund, 2003
pre-planorbis beds
C. marshii zone
Sevatian 2 R. suessi zone
Eiberg Basin
von Hillebrandt et al., 2007
P. spelae zone
pre-planorbis/ Schattwald beds
C. marshii zone
NW Europe
Hettangian (Lias)
Uppermost Rhaetian
Rhaetian
Norian
Warrington et al., 2008
Psiloceras planorbis zone
pre-planorbis beds
Lilstock Fm
Westbury Fm
Blue Anchor Fm
Williton Mb
Rydon Mb
Twyning Mudstone
Germanic Basin
Tethys realm
This study
Hettangian (Lias)
Uppermost Rhaetian
Rhaetian
Jurassic palynological flora
Triletes-beds/ transition zone
Contorta-beds/ Haupt-ton
Haupt Sandstein/ Postera-beds
P. spelae tirolicum zone
Schattwald beds
Eiberg Member (Kössen Formation)
Choristoceras zone

Figure DR1

Fig. DR2

Wuestenwelsberg section: $\delta^{13}C_{Leaf}$
(Germanic basin/ Germany)

Sample no.	Sample depth (cm)	$\delta^{13}C_{Leaf}$	$\delta^{13}C_{Leaf}$ (average/ level)
WZ-58-A-A	652	-26,03	-26,2
WZ-58-B-A	652	-26,34	
WZ-53-A-A	707	-27,05	-27,0
WZ-53-B-A	707	-27,55	
WZ-53-C-A	707	-26,62	
WZ-53-D-A	707	-26,64	
K2a-A-A	720	-27,12	-27,1
K2a-B-A	720	-28,21	
K2a-C-B	720	-25,47	
K2a-D-A	720	-27,37	
K2a-E-A	720	-27,32	
K2o-A-A	744	-27,08	-27,6
K2o-B-A	744	-26,82	
K2o-C-A	744	-28,77	
K2o-D-A	744	-27,64	
WZ-57-A-A	753	-28,37	-27,4
WZ-57-B-A	753	-26,44	
K2b-A-A	763	-25,93	-26,6
K2b-B-A	763	-26,23	
K2b-C-A	763	-26,25	
K2b-D-A	763	-27,36	
K2b-E-A	763	-27,32	

Table DR1

Wuestenwelsberg section: $\delta^{13}C_{TOC}$
(Germanic basin/ Germany)

Sample no.	Sample depth (cm)	$\delta^{13}C_{TOC}$
WZ102	2035	-26,28
WZ101	2012	-26,57
WZ100	1990	-26,80
WBK-97	1443	-22,6
WBK-96	1433	-22,5
WBK-95	1426	-22,9
WBK-94	1420	-22,8
WBK-93	1411	-22,6
WBK-92	1401	-23,0
WBK-91	1387	-22,7
WBK-88	1334	-22,9
WBK-86	1315	-22,3
WBK-84	1294	-23,3
WBK-83	1285	-23,6
WBK-80	1255	-23,5
WBK-79	1233	-23,2
WBK-77	1209	-23,2
WBK-75	1184	-23,0
WBK-74	1175	-23,3
WBK-72	1150	-23,5
WBK-70	1129	-24,4
WBK-65	1066	-23,8
WBK-63	1040	-23,9
WBK-61	1020	-23,5
WBK-60	1008	-23,5
WBK-59	1002	-23,5
WBK-57	983	-23,6
WBK-53	948	-23,8
WBK-52	937	-23,5
WBK-49	897	-23,3
WBK-48	887	-23,3
WZ6	867	-23,5
WZ7	863	-24,2
WZ8	860	-23,7
WZ9	855	-24,4
WZ10	848	-25,8
WZ11	839	-24,6
WZ12	828	-24,2
WZ13	822	-25,7
WZ14	813	-25,5
WZ15	808	-24,7
WZ16	801	-24,3
WZ17	794	-24,2
WZ18	785	-24,6
WZ19	776	-24,7
WZ20	770	-24,9
WZ21	763	-24,6
WZ22	756	-25,4
WZ23	752	-26,4
WZ24	750	-26,6
WZ25	746	-26,9
WZ26	743	-26,6
WZ27	739	-26,3
WZ28	733	-26,1
WZ29	729	-25,5
WZ30	723	-23,9
WZ31	719	-24,6
WZ32	714	-24,8
WZ33	710	-25,7
WZ34	705	-25,3
WZ35	699	-25,3
WZ36	694	-25,0
WBK-32	684	-24,2
WBK-30	668	-24,3
WBK-28	652	-24,9
WBK-26	626	-24,5
WBK-24	592	-25,1
WBK-22	570	-25,1
WBK-20	539	-25,1
WBK-18	515	-25,1
WBK-17	505	-25,1
WBK-15	478	-24,9
WBK-13	435	-24,8
WBK-11	405	-25,0
WBK-9	343	-24,9
WBK-7	341	-24,7
WBK-6	331	-24,5
WBK-4	319	-24,4
WBK-3	304	-24,4
WBK-2	287	-24,0
WW15	170	-24,5
WW 14	164	-24,7
WW13	156	-24,5
WW12	144	-24,0
WW11	130	-24,3
WW10	122	-24,6
WW9	114	-24,4
WW8	110	-24,6
WW7	106	-24,6
WW6	102	-25,1
WW5	98	-24,7
WW4	93	-24,6
WW3	89	-24,7
WW2	83	-24,4
WW1	77	-24,4

Eiberg section: $\delta^{13}C_{TOC}$
(Eiberg basin/ Austria)

Sample no.	Sample depth (cm)	$\delta^{13}C_{TOC}$
Eib 1	791	-31,4
Eib 2	790	-29,9
Eib 3	789	-30,5
Eib 4	786	-31,2
Eib 5	785	-31,6
Eb 6	784	-31,3
Eib 7	783	-30,2
Eib 8	781	-29,9
Eib 9	779,5	-28,5
Eib 10	776	-27,9
Eib 11	771	-27,8
Eib 12	766	-27,4
Eib 13	766	-25,9
Eib 14	696	-26,5
Eib 15	596	-25,8
Eib 16	536	-25,9
Eib 17	496	-25,6
Eib 18	471	**-26,4**
Eib 19	451	-25,7
Eib 20	436	-25,7
Eib 21	416	-25,7

EI 1	488	-26,5
EI 2	487	-26,7
EI 3	486	-26,7
EI 4	484	-26,9
EI 5	482	-27,0
EI 6	471	**-26,9**
EI 7	460	-27,1
EI 8	450	-26,7
EI 9	438	-26,3
EI 10	426	-26,5
EI 11	413	-26,6
EI 12	403	-26,7
EI 13	386	-26,6
EI 14	376	-26,6
EI 15	369	-26,8
EI 16	358	-26,7
EI 17	348	-26,8
EI 18	335	-26,9
EI 19	326	-27,8
EI 20	315	-27,9
EI 21	306	-27,6
EI 22	298	-27,2
EI 23	288	-27,0
EI 24	279	-26,4
EI 25	273	-26,5
EI 26	269	-26,3
EI 30	264	-26,7
EI 31	254	-26,7
EI 32	244	-26,7
EI 33	237	-27,3
EI 34	230	-29,9
EI 35	228	-27,8
EI 36	219	-27,9
EI 37	210	-28,2
EI 38	200	-27,2
EI 39	192	-27,4
EI 40	186	-27,9
EI 41	181	-28,4
EI 42	170	-29,6
EI 43	164	-29,1
EI -1	157	-26,9
EI -2	151	-26,7
EI -3	145	
EI -4	142	-26,53
EI -5	133	-26,73
EI -6	123	-26,86
EI -7	110	-27,54
EI -8	98	-27,36
EI -9	84	-27,49
EI -10	76	-27,31
EI -33	69	-27,62
EI -34	50	-27,51
EI -35	41	-27,26
EI -36	33	-27,05
EI -37	28	-27,75
EI -38	18	-27,40
EI -39	10	-27,23
EI -40	2	-26,92

REFERENCES CITED

Bachmann, G., and Kozur, H.W., 2004, The Germanic Triassic: correlations with the international chronostratigraphic scale, numerical ages and Milankovitch cyclicity: Hallesches Jahrbuch Geowissenschaften, v. B 26, p. 17-62.

Beerling, D.J., and Berner, R.A., 2002, Biogeochemical constraints on the Triassic-Jurassic boundary carbon cycle event: Global Biogeochemical Cycles, v. 16.

Bloos, G., 1990, Eustati sea-level changes in the upper Keuper and in the lower Lias of Central Europe: Cahiers Univ. Catho. Lyon, ser. Sci., v. 3, p. 5-16.

Bocherens, H., Friis, E.M., Mariotti, A., and Raunsgaard Pedersen, K., 1993, Carbon isotopic abundances in Mesozoic and Cenozoic fossil plants: Palaeoecological implications: Lethaia, v. 26, p. 347-358.

Bonis, N.R., Kürschner, W.M. and Krystyn, L., 2009. A detailed palynological study of the Triassic-Jurassic transition in key sections of the Eiberg Basin (Northern Calcareous Alps, Austria). Review of Palaeobotany and Palynology, 156(3-4): 376-400, doi: 10.1016/ j.revpalbo.2009.04.003.

Bonis, N.R., Ruhl, M. and Kürschner, W.M., 2010. Climate change driven black shale deposition during the end-Triassic in the western Tethys. Palaeogeography, Palaeoclimatology, Palaeoecology, 290(1-4): 151-159.

Bonis, N.R., Van Konijnenburg-Van Cittert, J.H.A. and Kürschner, W.M., in press. Changing CO2 conditions during the end-Triassic inferred from stomatal frequency analysis on Lepidopteris ottonis (Goeppert) Schimper and Ginkgoites taeniatus (Braun) Harris. Palaeogeography, Palaeoclimatology, Palaeoecology, In Press, Accepted Manuscript.

Chanell, J.E.T., Kozur, H.W., Sievers, T., Mock, R., Aubrecht, R., and Sykora, M., 2003, Carnian-Norian biomagnetostratigraphy at Silicka Brezova (Slovakia): correlation to other Tethyan sections and to the Newark Basin: Palaeogeography, Palaeoclimatology, Palaeoecology, v. 191, p. 65-109.

Hillebrandt, A., Krystyn, L., and Kürschner, W.M., 2008, A candidate GSSP for the base of the Jurassic in the Northern Calcareous Alps (Kuhjoch section, Karwendel Mountains, Tyrol, Austria): International Subcommission on Jurassic Stratigraphy Newsletter, v. 34, p. 2-20.

Hillebrandt, A.v. and Krystyn, L., 2009. On the oldest Jurassic ammonites of Europe (Northern Calcareous Alps, Austria) and their global significance. N. Jb. Geol. Palaeont. Abh., 253(2-3): 163-195.

Kozer, H.W., 2003, Integrated ammonoid, conodont and radiolarian zonation of the Triassic and soem remarks to Stage/ Substage subdivision and the numeri age of the Triassic stages: Albertiana, v. 28, p. 57-74.

Krystyn, L., Richoz, S., Gallet, Y., Bouquerel, H., Kurschner, W.M., and Spotl, C., 2007, Updated bio- and magnetostratigraphy from Steinbergkogel (Austria), candidate GSSP for the base of the Rhaetian stage: Albertiana, v. 36, p. 164-173.

Kürschner, W.M., Bonis, N.R., and Krystyn, L., 2007, Carbon-isotope stratigraphy and palynostratigraphy of the Triassic-Jurassic transition in the Tiefengraben section -- Northern Calcareous Alps (Austria): Palaeogeography, Palaeoclimatology, Palaeoecology, v. 244, p. 257-280.

Lund, J.J., 2003, Rhaetian to Pliensbachian palynostratigraphy of the central part of the NW German Basin exemplified by the Eitzendorf 8 well: Courier Forschungs-Institut Senckenberg, v. 241, p. 69-83.

Nitsch, E., Seegis, D., Vath, U., and Hauschke, N., 2005, Sedimente und Sedimentationspausen im deutschen Keuper: Wie vollstandig ist die Uberlieferung der spaten Triaszeit?: Newsl. Stratigr., v. 41, p. 225-251.

Ruhl, M., Kürschner, W.M., and Krystyn, L., 2009, Triassic-Jurassic organic carbon isotope stratigraphy of key sections in the western Tethys realm (Austria): Earth and Planetary Science Letters, v. 281, p. 169-187.

Sun, B., Dilcher, D.L., Beerling, D.J., Zhang, C., Yan, D., and Kowalski, E., 2003, Variation in Ginkgo biloba L. leaf characters across a climatic gradient in China: PNAS, v. 100, p. 7141-7146.

Warrington, G., Cope, J.C.W., and Ivimey-Cook, H.C., 2008, The St. Audrie's Bay - Doniford Bay section, Somerset, England: updated proposal for a candidate Global Stratotype Section and Point for the base of the Hettangian Stage, and of the Jurassic System: International Subcommission on Jurassic Stratigraphy Newsletter, v. 35, p. 2-66.